

**INFLUENCE OF RE-ENTRAINMENT AND CHARGED PARTICLES
ON PARTICLE DEPOSITION ONTO DOWNSTREAM WALL
IN AN ELECTROSTATIC PRECIPITATOR**

K.YASUMOTO*, A. ZUKERAN*, T. KIMURA, K. ITO**, K. YUDA**,
Y. TAKAGI** AND Y. EHARA****

***Fuji Electric Systems Co., Ltd., Japan**

****Musashi Institute of Technology, Japan**

ABSTRACT

One application of an electrostatic precipitator (ESP) is decontaminating polluted gases in expressway tunnels to save drivers and environment around tunnels. High collection efficiency is well achieved by a conventional ESP. However, the walls downstream the ESP are polluted due to particle deposition. Although it was thought that the cause was the emission of charged particles from the ESP, authors thought that one of the causes was also particle re-entrainment on the ESP. In this paper, the experiments were carried out to investigate the effect of neutralization on preventing particle deposition. The collection efficiency as a function of particle diameter and the amount of deposited particles on the wall were studied on three types of the ESP, which were the universal ESP under DC operating mode (DCESP), the ESP under AC operating mode (ACESP) and the ACESP with neutralization. The ACESP is new type that is developed to prevent the particle re-entrainment by authors. The results showed that the collection efficiency of a large particle decreased on the DCESP because of the particle re-entrainment. Although the amount of deposited particles on the DCESP was the greatest, that on the ACESP was low due to preventing particle re-entrainment. The ACESP with neutralizer was most effective to decrease the amount of deposited particles of three types of the ESP, because of the preventing particle re-entrainment and the decreasing the charge amount of gases downstream the ACESP with the neutralization.

INTRODUCTION

An electrostatic precipitator (ESP) has been extensively used for cleaning of industrial process flue gases, combustion flue gases, and ventilation flue gases of buildings, etc., because of its high collection efficiency. One of the applications of ESP is decontaminating polluted gases and improves the visibility index in road tunnels to save the air environment around tunnels and drivers.

In generally, the high collection efficiency between 0.01 to 10 μm on an ESP is achieved. However, the collection efficiency of sub-micron particles, whose size is between 0.1 to 1 μm , is lower than that of the others [1]. Therefore, the efficiency of the ESP in collecting submicron particles has been investigated. The collection efficiency in the ESP to remove the particles with a high resistivity decreases due to the back corona [1][2]. On the other hand, it is very important to prevent the particle re-entrainment for the ESP for road tunnels to remove the particles with a low resistivity [3].

There is the problem, which is particle deposition onto walls downstream the ESP for road tunnels. The watching performance at tunnel observation points decreases due to particle deposition on cameras, lights and walls, etc.. It also spoils the beauty of surround a tunnel. One of the causes is that particles downstream ESP are charged [4]. However, the authors have been investigated the influence of particle re-entrainment on particle deposition. As the results, it is clear that the particle re-entrainment influent on particle deposition onto walls. The particle deposition decreased when the particle re-entrainment was prevented by ESP under AC operating mode (ACESP) [5].

In this paper, the experiment were carried out to clear the effect of neutralizing the gases downstream ACESP on decreasing more the particle deposition. There were three types in experimental ESP, which were ESP under DC operating mode (DC ESP), ACESP and ACESP with neutralizer.

1. EXPERIMENTAL

2.1 Summary Of Experimental System

The schematic of experimental system used in the present work is shown in Fig.1. The gases exhausted from the diesel engine are diluted with air in the mixing chamber, then boosted by the fan and introduced into the ESP system. The gases cleaned by ESP pass through an absorbing fan, and are then exhausted. The gas velocity in the duct is approximately 5 m/s.

2.2 ESP Arrangement And Sampling Location

The schematic of the ESP is shown in Fig.2. The two-stage type ESP consists of the precharger and the collector. The precharger consists of wires and plates. The wires of

tungsten were 0.26 mm in diameter, and the plates were made of aluminum. The collector had a parallel-plates configuration and the spacing between adjacent plates was 9mm.

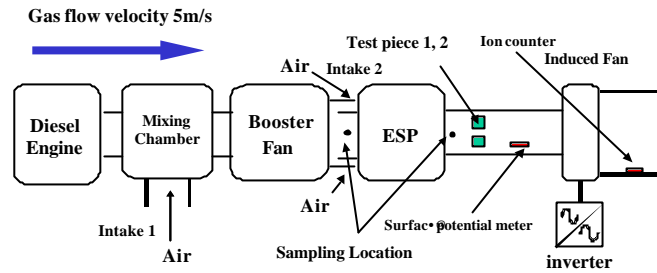


Figure 1: Schematic of experimental system

The applied voltage arrangement of each ESP is shown in Table 1. Negative DC high voltage was applied to the precharger and the collector in the DCESP. Negative corona discharge is used to charge particles in the precharger. The charged particles are collected on the electrodes in the collector. Negative DC high voltage was applied to the precharger, and the AC high voltage is applied to the collector in the ACESP. Negative DC high voltage is applied to the discharge wire electrode NO.1, and positive DC high voltage is applied to the discharge wire electrode NO.2 of the precharger in ACESP with the neutralization. AC high voltage was applied to the collector. The gases

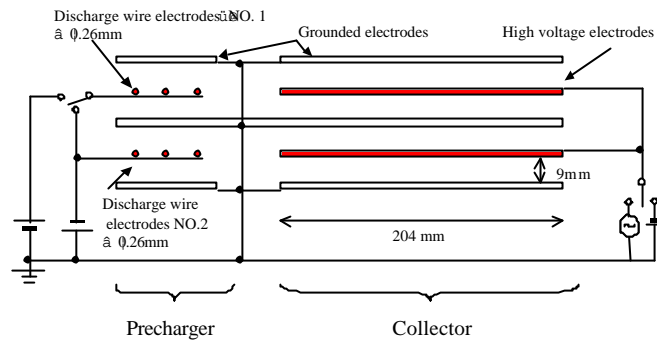
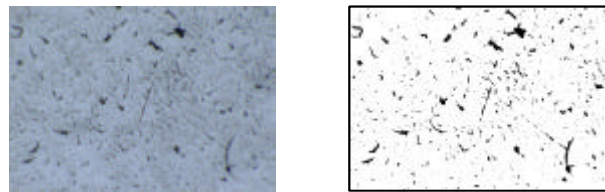


Figure 2: Schematic of electrostatic precipitator



a) microscope photograph b) 2-step gradation

Figure 3: Image processing

included the charged particles and the ions downstream ACESP with the neutralization is

Table 1: Applied voltage arrangement

	Precharger (discharge wire electrode)				Collector
	NO.1		NO.2		
	Voltage	Corona current	Voltage	Corona current	Voltage
DCESP	DC -10.0 kV	0.65mA	DC -10.0 kV	0.65 mA	DC -8 kV
ACESP	DC -10.0 kV	0.65 mA	DC -10.0 kV	0.65 mA	AC 8 kV
ACESP with neutralization	DC -10.0kV	0.65 mA	DC +11.6kV	0.65 mA	AC 8kV

neutral, because

of mixing the negative charged particles and the positive charged particles. The ESP operating time was 60 min, respectively.

The particle counter (PC; RION, model KC-01C) measures the number concentration of particles larger than 0.3 μm in real-time at the upstream and the downstream of ESP as shown in Fig.2. The collection efficiency η is calculated by equation (1),

$$\eta = \frac{N_U - N_D}{N_U} \cdot 100 \quad (1)$$

where N_U is the particle concentration of upstream of ESP, N_D is that of downstream.

The test pieces 1 (TOUBE, DC#200) and 2 (aluminum foil) were attached in the duct downstream the ESP. The particle deposit rate α on the test piece 1 was measured by the optical microscope (KEYENCE, VH-7000). The deposited particles on the test piece 2 were observed by the scanning electron microscope (SEM, HITACHI, S-4100). The images of the optical microscope were processed to the two-step gradation as shown in Fig.3, and the particle deposition rate α was defined as

$$a = \frac{S_b}{S} \cdot 100 \quad (2)$$

where as S is the number of total dots of images, S_b is the number of black area dots of images.

2.3 Measurement Of Surface Potential And Ion Concentration

The surface potential was measured to evaluate the charging amount of the gases downstream the ESP. The measurement system of surface potential is shown in Fig.4. The metal plate, which was insulated, was installed in the duct downstream the ESP. The surface potential of the metal plate was measured by the surface potential meter (TREK, Model 344).

The surface potential cannot measure the concentration of the negative and the positive ion individually. The negative and the positive ion concentrations were measured to investigate the effect of the ACESP with the neutralization. The ion counter (ANDES, ITC-201A) was installed in the duct as shown in Fig.1. The ion counter can measure the ion concentration

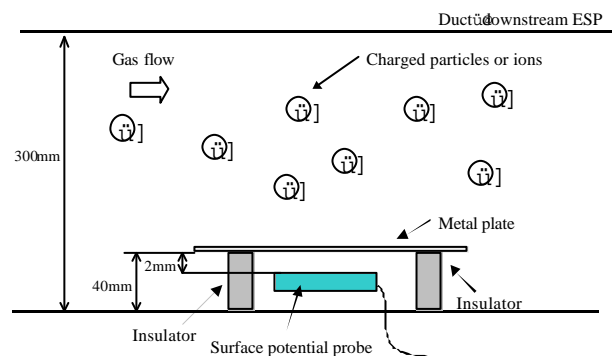


Figure 4: Measurement system of surface potential

for the mobility of $0.6 \text{ cm}^2/(\text{V sec})$.

3. RESULTS AND DISCUSSIONS

3.1 Collection Efficiency Of ESP

The collection efficiency as a function of particle diameter in each ESP is shown in Fig.5. The collection efficiency for particles of $0.3\text{-}1 \mu\text{m}$ are almost same, respectively. The collection efficiency in DCESP decreases with the increasing particle diameter, and is negative collection efficiency for particle of $2\text{-}5 \mu\text{m}$ due to the particle re-entrainment. On the other hand, the collection efficiency for the particle of $1\text{-}5 \mu\text{m}$ in the ACESP and the ACESP with neutralization are significantly improved, because of the preventing particle re-entrainment.

3.2 Particle Deposition Rate Of ESP

The particle deposition rate in each ESP is shown in Fig.6. The particle deposition rate is 2.2% for DCESP, 0.48% for the ACESP and 0.11% for ACESP with the neutralization. The particle deposition rate in the ACESP is less than that in DCESP. It is clear that the ACESP with the neutralization is most effective to decrease the particle deposition rate.

The SEM images of deposited particles in each ESP are shown in Fig.7. The fine particles and large particles are observed in DCESP as shown in Fig.7 (a). The large particles are not observed in ACESP due to the effect of the preventing particle re-entrainment, however, the fine particles are observed as shown in Fig.7 (b). Both of the fine particles and large particle are not observed in ACESP with the neutralization as shown in Fig.7 (c).

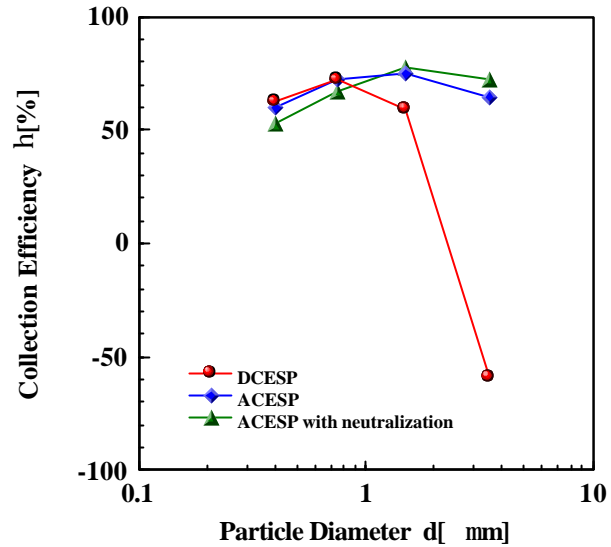


Figure 5: Collection efficiency as a function of particle diameter

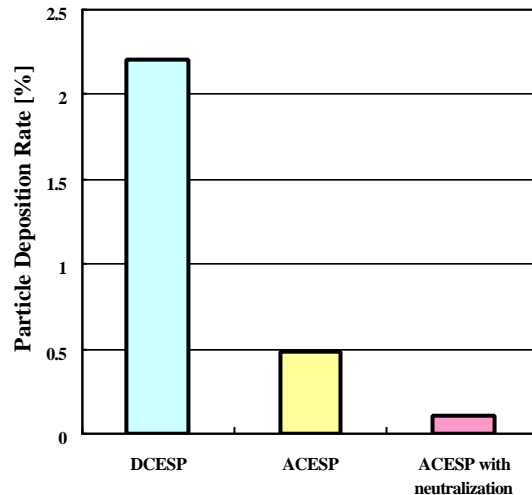
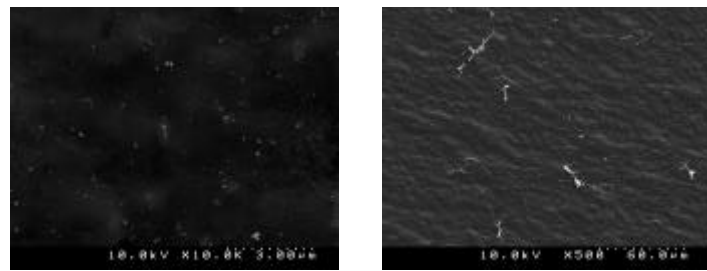


Figure 6: Particle deposition rate for various ESP

3.3 Model of Particle Deposition And Re-entrainment

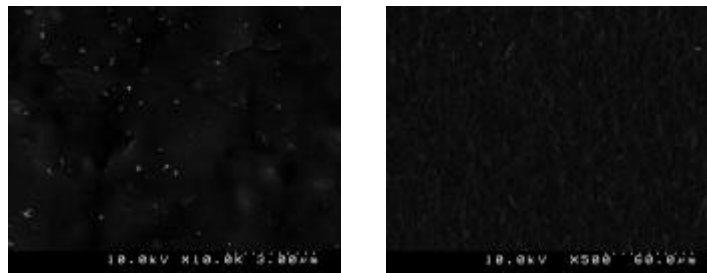
The model of the particle deposition in the DCESP is shown in Fig.8. The particles are charged in the precharger, and collected on the electrodes in the collector. The agglomerated particles like a pearl chain are generated on the electrodes, and the pearl chain particles emit to the duct downstream the DCESP. The penetrating charged fine particles and re-entrained large particles deposit onto the walls due to Coulomb force.



High magnification

Low magnification

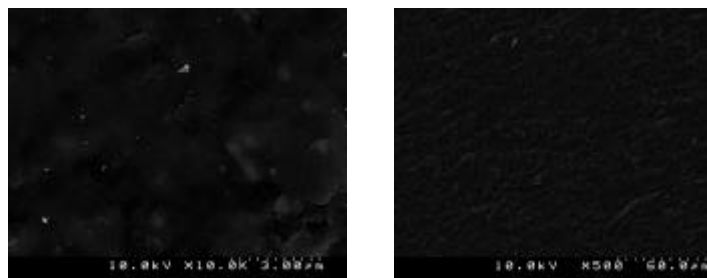
a) DCESP



High magnification

Low magnification

b) ACESP



High magnification

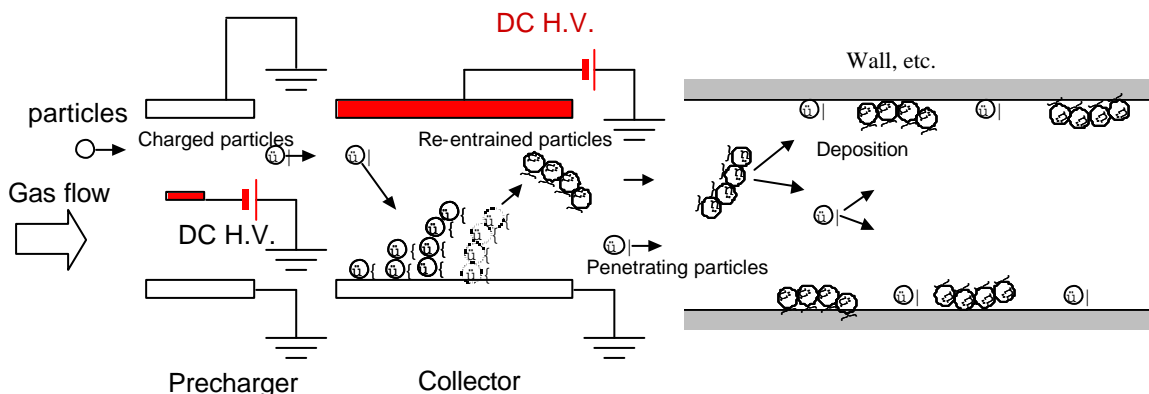
Low magnification

c) ACESP with neutralization

Figure 7: SEM images of deposited particles on the wall

The model of the preventing re-entrainment in ACESP is shown in Fig.9. (a) The particles charged negatively in the precharger are collected on the positive electrode in the collector. The collected particles are re-charged same polarity with collected electrodes and agglomerate like a pearl chain. (b) The shape of pearl chain particles changes to the spherical, when the electric field changes. The spherical particles have large contact area between the particle and the electrode. Therefore, the particle re-entrainment is prevented in the ACESP due to increasing the adhesion force

The spherical particles have large contact area between the particle and the electrode. Therefore, the particle re-entrainment is prevented in the ACESP due to increasing the adhesion force



between the particle and the electrode.

The gases included the charged particles and the ions are neutral in ACESP with the neutralization, so that the particles are charged both negatively and positively as shown in Fig.2 and Table 1. In addition, the particle re-entrainment is prevented. Therefore, the ACESP with the neutralization is most effective to decrease the particle deposition rate.

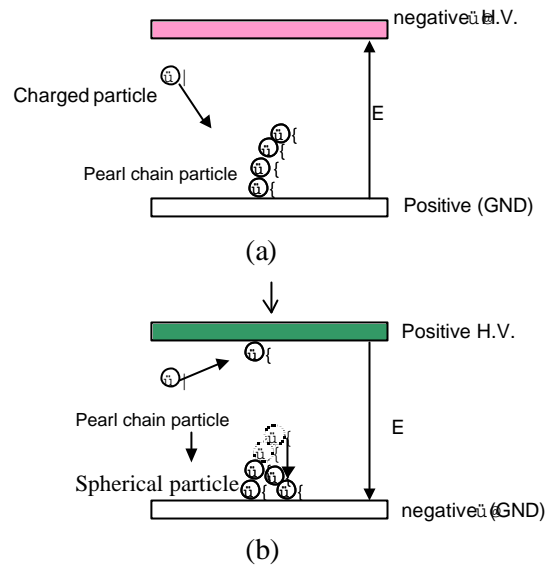


Figure 9: Model of preventing particle re-entrainment in the ACESP

3.4 Surface Potential And Ion Concentration Downstream ESP

The surface potential and the ion concentration in each ESP is shown in Table 2. The surface potential is -279V for the DCESP, -136V for the ACESP and -12V for the ACESP with the neutralization. It is clear that the gases downstream the ACESP with the neutralization is neutral compared with another ESP.

The precharger in the ACESP with the neutralization has the positive corona part and the negative corona part. Therefore, the plus ion concentration in the ACESP with the neutralization is greater than that in the DCESP and the ACESP. The minus ion concentration in the ACESP with the neutralization is approximately $1/2$ compared with that in the DCESP and the ACESP. The total ion concentration in the ACESP with the neutralization is 43130 part/cm^3 compared with 57230 part/cm^3 for the DCESP and 50770 part/cm^3 for the ACESP. Therefore, that there are both the plus ions and the minus ions in the ACESP with the neutralization.

Table 2: Surface potential and ion concentration downstream ESP

	Surface potential [V]	Ion concentration [part/cm ³]		
		+ ion	- ion	Total
DCESP	-279	0	57230	57230
ACESP	-136	230	50540	50770
ACESP with neutralization	-12	12660	30470	43130

These results indicate that the charge amount in the gases downstream the ACESP with the neutralization is almost neutral so that there are the plus ion and the minus ion in the gases

individually. Most of the plus ions do not combine with the minus ions.

4. CONCLUSION

The experimental was carried out to clear the effect of ACESP with the neutralization on the particle deposition on the wall downstream the ESP. The results are follows;

1. The ACESP and the ACESP with the neutralization prevented the particle re-entrainment compared with the DCESP.
2. The fine particles and the large particles are observed in the DCESP.
3. The large particles were not observed on the walls in ACESP due to preventing the particle re-entrainment. Therefore, the amount of particle deposition on the wall in the ACESP decreases compared with that in the DCESP.
4. The gases downstream the ACESP with neutralization was almost neutral. Therefore, the large particles and the fine particles are not observed in the ACESP with the neutralization. The ACESP with the neutralization was most effective to prevent the particle deposition of three types of ESP.
5. The charge amount in the gases downstream the ACESP with the neutralization is almost neutral so that there are the plus ions and the minus ions individually. Most of the plus ions do not combine with the minus ions.

AKNOWLEDGMENT

The authors wish to thank Prof. T.Ito, Prof. T.Takahashi, Musashi Institute of Technology, Tokyo, Japan, and Y.Kono, Fujielectric systems co., ltd., Japan, for valuable comments and discussions.

REFERENCES

- [1] Jen-shih Chang, Arnold J.Kelly, Joseph M. Crowley, "Handbook of electrostatic process", Marcel Dekker, Inc., 1995
- [2] T.Misaka, A.Akasaka, T.Oura, M.Hirano, H.Asano, "Electrostatic precipitator combined pulse charging section with moving electrode section for high resistivity dust", Proceeding of 6th International conference on electrostatic precipitation, 45-56, 1996
- [3] A.Zukeran, Y.Ikeda, Y.Ehara, M.Matsuyama, T.Ito, T.Takahashi, H.Kawakami, T.Takamatsu, "Two-stage-type electrostatic precipitator re-entrainment phenomena under diesel flue gases", IEEE Trans. Ind. Applicat., **35**, 346-351, 1999
- [4] T.Takahashi, T.Takamatsu, H.Kawakami, A.Zukeran, H.Fujimura, Y.Ehara, T.Ito, "Particle deposit on the surface of the wall by electrostatic precipitators", (In Japanese), The Journal of Institute of Electrical Installation Engineers of Japan, **18**, 853-859, 1998
- [5] K.Yasumoto, A.Zukeran, Y.Takagi, Y.Ehara, "Preventing re-entrainment and particle deposition in an electrostatic precipitator under AC operating mode", 41st Summer Symposium, The Society of Powder Technology, Japan, 45-50, 2005